

Application of new azomethine as corrosion inhibitor on mild steel in acidic medium: Electrochemical, thermodynamic and SEM investigations.

HAMANI Hanane

Laboratory of Electrochemistry of Molecular Materials and Complexes (LEMMC)

Department of Engineering Process, Faculty of Technology

University Setif 1, DZ-19000 Setif, Algeria

hanane.hamani@gmail.com

DOUADI Tahar

Laboratory of Electrochemistry of Molecular Materials and Complexes (LEMMC)

Department of Engineering Process, Faculty of Technology

University Setif 1, DZ-19000 Setif, Algeria

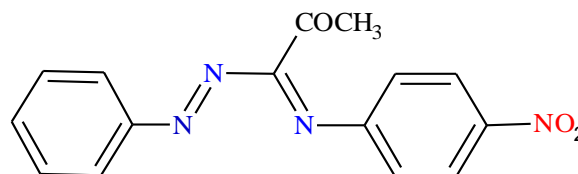
daouadi.tahar@gmail.com

Abstract—1-(4-Nitrophenyl-imino) -1 (phenylhydrazono) -propan-2-one (NO₂AM) was studied as a corrosion inhibitor for the protection of mild steel in 1 M HCl solution by means of weight loss, polarization and electrochemical impedance spectroscopy. The inhibition efficiency was found to increase with increasing inhibitor concentrations and decreases with increasing temperatures. Some thermodynamic and kinetic parameters were calculated and discussed. The adsorption of inhibitor on mild steel surface, obeyed the Langmuir adsorption isotherm. Polarization studies showed that inhibitor behave as mixed-type inhibitor. Scanning electron microscopy (SEM) was performed for surface analysis of the uninhibited and inhibited mild steel samples.

Keywords— Corrosion, Inhibition, Electrochemical, SEM.

Introduction

A corrosion inhibitor is often added to mitigate the corrosion of metal by acid attack. Most well-known corrosion inhibitors are organic compounds containing polar groups including nitrogen, sulfur, and/or oxygen atoms and heterocyclic compounds with polar functional groups and conjugated double bonds. These substances generally become effective by adsorption on the metal surface. The adsorbed species protect the metal from the aggressive medium, which causes decomposition of the metal. Adsorption depends on not only the nature and charge of the metal but also on the chemical structure of the inhibitor [1–6]. The objective of the present work is to investigate inhibitive efficiency of azomethine : 1-(4-Nitrophenyl-imino) -1 (phenylhydrazono) -propan-2-one (NO₂AM) [7] for mild steel in 1 M HCl solution using potentiodynamic polarisation, electrochemical impedance spectroscopy, and SEM method. The Scheme 1, show the chemical structure of the azomethine compound (NO₂AM).



Scheme. 1. The chemical structure of 1-(4-Nitrophenyl-imino) -1 (phenylhydrazono) -propan-2-one (NO₂AM).

I. EXPERIMENTAL

A. Material and sample preparation

The mild steel specimen having the chemical composition (wt %): C = 0.39; P = 0.024; Si = 0.23; Mn = 0.78; Cr = 0.14; Cu = 0.20; Al = 0.023; Ni = 0.23; Mo = 0.030 and the rest is Fe, is used in this study. The test solution 1 M HCl is prepared by dilution of analytical grade 37% HCl solution with distilled water. The concentration of the corrosion inhibitor is kept in the range of 5×10^{-6} - 7.5×10^{-5} M.

B. Electrochemical measurements

Electrochemical studies were conducted in a three-electrode cell consisting of mild steel specimen of 0.19 cm² exposed area as working electrode, a platinum counter electrode and a saturated calomel electrode (SCE) as reference electrode. Prior to each electrochemical test the working electrode is immersed in the test solution for about 30 min to attain open circuit potential (EOCP) at 25°C. Potentiodynamic polarization curves were obtained at a scan rate of 0.5 mV/S in the potential range of -800 to -250 mV vs. SCE at open circuit potential (EOCP). The linear Tafel segments of anodic and cathodic curves were extrapolated to obtain corrosion current densities (*i*_{corr}). The inhibition efficiency (EIP%) and surface coverage (θ) are determined by using the following equations [8] :

$$EI_P \% = \left(\frac{i_{corr}^{\circ} - i_{corr}}{i_{corr}} \right) \times 100 \quad (1)$$

$$\theta = \frac{i_{corr}^{\circ} - i_{corr}}{i_{corr}} \quad (2)$$

where i_{corr}° and i_{corr} are the corrosion current densities in the absence and presence of inhibitors, respectively. The electrochemical impedance measurements (EIS) were performed in the frequency range of 100 kHz to 10 mHz with at 10 mV amplitude at the open circuit potential (EOCP). The inhibition efficiency (EISIE%) was calculated from charge transfer resistance values obtained from impedance measurements using the following equation [9]:

$$EI_{SIE} \% = \frac{R_{ct_0}^{-1} - R_{ct}^{-1}}{R_{ct_0}^{-1}} \times 100 \quad (3)$$

where R_{ct}° and R_{ct} are charge transfer resistance in the absence and presence of inhibitor, respectively. The values of double layer capacitance (Cdl) were calculated from charge transfer resistance and CPE parameters (Q and n) using the equation [9]:

$$C_{dl} = (Q R_{ct}^{1-n})^{1/n} \quad (4)$$

Where Q is CPE constant and n is CPE exponent. The value of n represents the deviation from the ideal behavior and it lies between 0 and 1. Potentiodynamic polarisation and electrochemical impedance spectroscopy (EIS) experiments were carried out using a PGZ 301 voltalab 40 model potentiostat/galvanostat.

C. Scanning electron microscopic (SEM)

For surface morphological study of the uninhibited and inhibited mild steel samples, SEM images were recorded using the instrument JOEL-JSM-7001F-Japan.

II. RESULTS AND DISCUSION

A. Potentiodynamic polarization curves

Fig. 1 show the potentiodynamic polarization curves for mild steel in 1 M HCl solution in the absence and presence of different concentrations of azomethine (NO_2AM). The electrochemical parameters such as corrosion potential (E_{corr}), corrosion current density (i_{corr}), corrosion inhibition efficiency (EI_P), anodic Tafel slope (B_a) and cathodic Tafel slope (B_c) were derived from extrapolation method and represented in Table 1.

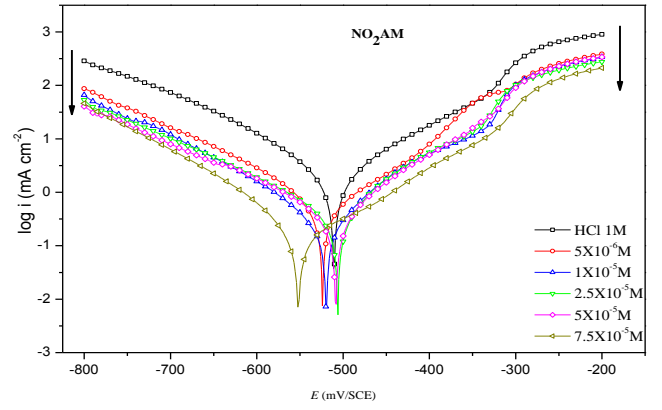


Fig.1. Potentiodynamic polarization curves of mild steel in 1 M HCl solution without and with different concentrations of NO_2AM at 25 °C.

It can be clearly found in Fig. 1 that both cathodic and anodic current densities decrease distinctly when the NO_2AM is added in the acid solution, and the variations of cathodic current densities with inhibitor concentrations are more noticeable. Namely, anodic metal dissolution and cathodic hydrogen evolution reactions are markedly inhibited by the NO_2AM compound, and the inhibiting effect becomes more pronounced with gradual increase of the inhibitor concentrations, and there is no distinct trend in the shift of E_{corr} values. The observation is very much clear with NO_2AM inhibitor, showing almost coinciding corrosion potentials and hence may be treated as mixed inhibitor. The displacement in E_{corr} value in the absence and presence of the inhibitor, were less than 85 mV which states that the inhibitors is mixed type [10, 1]. Besides, it can be found that the cathodic branches of the polarization current-potential curves give rise to Tafel lines that are almost parallel. This phenomenon indicates that the addition of the inhibitor does not modify the hydrogen evolution mechanism, and most probably the reduction of hydrogen ions on the mild steel surface takes place mainly through a charge transfer mechanism [11, 3]. The adsorbed inhibitor molecules only block the active sites of hydrogen evolution on the metal surface. In anodic domain, it shows that the slopes of the anodic Tafel curves change little before and after addition of the inhibitor to the hydrochloric acid solution, which means that the presence of the inhibitor does not change anodic dissolution mechanisms of the steel. However, the anodic current-potential curves display a slight deviation from linearity over the studied potential range, which may be due to the deposition of corrosion products on metal surface to form an uneven passive film [11]. As it can be seen from Table 1,

when the concentration of inhibitor increases the inhibition efficiencies increase while corrosion current densities decrease. It may be due to adsorption of inhibitor molecules on the metal surface. On increasing inhibitor concentration more no of inhibitor molecules adsorb and block the active sites of the metal surface. The maximum inhibition efficiency was observed around 96.06 % at $7.5 \times 10^{-5} \text{M}$ of the azomethine NO_2AM .

TABLE 1 Polarization curve parameters for the corrosion of mild steel in 1 M HCl solution without and with different concentrations of NO_2AM at 25 °C.

Inhibitor	C (M)	$-E_{corr}$ (mV/S CE)	$-B_c$ (mV /dec)	B_a (mV/d ec)	i_{corr} (mA cm ⁻²)	EI_p (%)	θ
	Blanc	510,6	63,7	65,4	0,515	-	-
NO_2AM	5×10^{-6}	523,9	74,9	89,3	0,101	80,31	0,80
	1×10^{-5}	519,8	79,4	73,0	0,065	87,33	0,87
	$2,5 \times 10^{-5}$	506,3	84,7	59,1	0,047	90,86	0,90
	5×10^{-5}	508,5	75,2	57,9	0,041	92,01	0,92
	$7,5 \times 10^{-5}$	551,8	85,3	74,3	0,038	92,63	0,92

Electrochemical impedance spectroscopy (EIS)

B. Electrochemical impedance spectroscopy (EIS)

The Nyquist plots for mild steel in 1M HCl solution in the absence (blank) and presence of different concentrations of NO_2AM at 25 °C are shown in Fig. 2. It can be observed that all the impedance spectra obtained show a single depressed capacitive loop which is related to charge transfer of the corrosion process [5] and the diameters of the capacitive loops increase sharply with increasing NO_2AM concentration. It is noticed that the impedance loops do not yield perfect semicircle. Such phenomenon is generally attributed to the frequency dispersion as well as heterogeneous roughness of metal surface and mass transfer process [6].

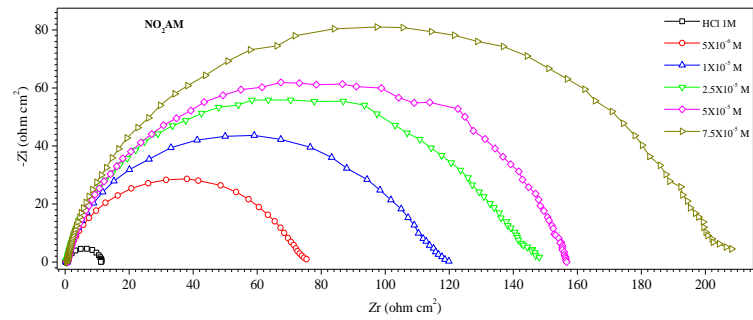


Fig.2. Nyquist plots for mil steel in 1 M HCl solution without and with different concentrations of of NO_2AM at 25 °C.

The electrochemical parameters obtained from the fitting of the impedance spectra are presented in Table 2. The data shown in Table 2 reveal that the R_{ct} values in the presence of inhibitor is larger than the R_{ct} for the blank. The increase in R_{ct} values is attributed to the formation of insulating protective film of the inhibitor at the metal/solution interface.

TABLE 2 EIS parameters for the corrosion of mild steel in 1 M HCl solution without and with different concentrations of NO_2AM at 25 °C.

Inhibit or	C (M)	R_s (Ωcm^2)	R_{ct} (Ωcm^2)	CPE	n	Q ($\mu \cdot \text{S}^n \cdot \Omega^{-1} \cdot \text{cm}^{-2}$)	C_{dl} ($\mu \text{F cm}^{-2}$)	EI_{SIE} (%)
	HCl	0,17	11,23	0,816		286,1	1764	-
NO_2AM	5×10^{-6}	0,53	73,20	0,884		74,33	229,5	84,65
	1×10^{-5}	0,51	115,8	0,889		46,84	136,5	90,30
	$2,5 \times 10^{-5}$	0,51	150,0	0,895		37,05	101,7	92,31
	5×10^{-5}	0,57	155,9	0,896		31,35	84,00	92,60
	$7,5 \times 10^{-5}$	0,45	205,9	0,892		21,68	59,95	94,54

From Table 2 it is observed that C_{dl} values decreased in the presence of inhibitors. This decrease in C_{dl} values might be due to a decrease in local dielectric constant and/or due to an increase in thickness of the double layer suggesting that inhibitors form a protective film mild steel surface in acid solution [2]. This decrease in C_{dl} value with increasing thickness of electric double layer can be explained using Helmholtz model [1]:

$$C_{dl} = \frac{\epsilon \epsilon_0 S}{d} \quad (5)$$

Where ϵ is the dielectric constant of the medium, ϵ_0 is the permittivity of the free space, S is the effective surface area of the working electrode, and d is the thickness of the electric double layer formed by the adsorb inhibitors. From the Helmholtz equation it can be concluded that increased in thickness of double layer was responsible for the decrease in Cdl values [3, 5].

C. Effect of temperature

In order to calculate the activation parameters of the corrosion process and the heat of adsorption process and to investigate the inhibition mechanism affected by temperature, polarization measurements were performed at various temperatures (25–55 °C), in the absence and presence of different concentration of NO_2AM . It is apparent that the increase of corrosion current density is pronounced with the rise of temperature in both uninhibited and inhibited solutions. The inhibition efficiency decreases slowly with increasing temperature. This type of behavior can be described on the basis that increase in temperature leads to a shift of the equilibrium position of the adsorption/desorption phenomenon towards desorption of the inhibitor molecules at the surface of mild steel [12].

The activation energy (E_a) of the corrosion process can be determined by the Arrhenius equation [13]:

$$i_{corr} = A \exp\left(\frac{-E_a}{RT}\right) \quad (6)$$

Where E_a is the activation energy of the corrosion process, T is the temperature, R is the gas constant, A is the Arrhenius constant and i_{corr} is corrosion current density. The Arrhenius plots of $\log i_{corr}$ vs $1/T$ of mild steel 1 M HCl solution is shown in Fig. 3 from which the values of E_a were calculated from the slope and listed in Table 3.

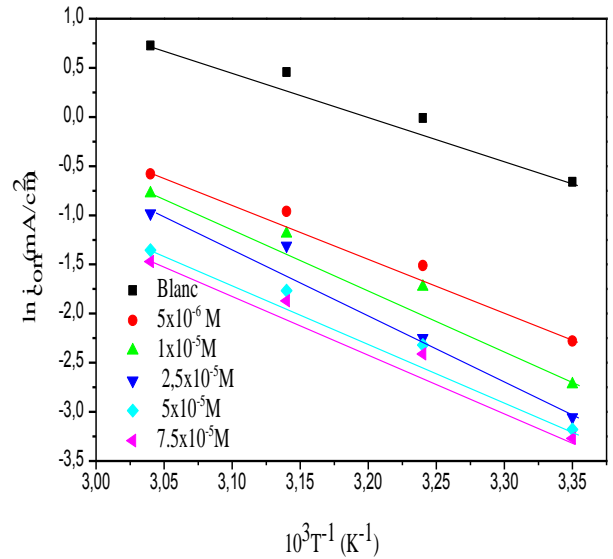


Fig. 3. Arrhenius plots for mild steel in 1M HCl in the absence and presence of different concentrations of NO_2AM .

TABLE 3 Activation parameters for mild steel in 1 M HCl in the absence and presence of different concentrations of SB and DBTDA.

Inhibitor	C(M)	E_a (KJ.mol ⁻¹)	ΔH_a° (KJ.mol ⁻¹)	ΔS_a° (J.mol ⁻¹)
	Blanc	37,97	28,134	-137,636
NO_2AM	5×10^{-6}	45,70	40,515	-128,307
	1×10^{-5}	51,06	43,955	-127,307
	$2,5 \times 10^{-5}$	57,83	46,767	-122,155
	5×10^{-5}	79,40	48,950	-114,306
	$7,5 \times 10^{-5}$	79,40	52,028	-109,583

The tabulated data revealed that value of E_a for inhibited solution is greater than that of uninhibited solution. This increase in E_a in presence of NO_2AM indicates the formation of higher energy barrier for corrosion process suggesting that adsorbed film of NO_2AM film on mild steel surface prevents the charge/mass transfer reaction occurring on the surface [12]. Moreover, the decrease in inhibition efficiency with increasing temperature signify the physical adsorption that occurs during first stage of adsorption process [13]. The increased value of E_a also suggest that presence of NO_2AM rate of mild steel dissolution decreased due to formation of metal-inhibitor complex [10].

The values of standard enthalpy of activation (ΔH_a°) and standard entropy of activation (ΔS_a°) were calculated by using Eq. (7):

$$i_{corr} = \frac{RT}{Nh} \exp\left(\frac{\Delta S_a^0}{R}\right) \exp\left(\frac{-\Delta H_a^0}{RT}\right) \quad (7)$$

where, h is Planck's constant and N is Avogadro's number, respectively.

A plot of $\ln(i_{corr}/T)$ against $1/T$ (Fig. 4) gave straight lines with a slope of $-\Delta H_a^0/R$ and an intercept of $[\ln(R/Nh) + (-\Delta S_a^0/R)]$, from which the value of activation thermodynamic parameters ΔH_a^0 and ΔS_a^0 were calculated, as listed in Table 3.

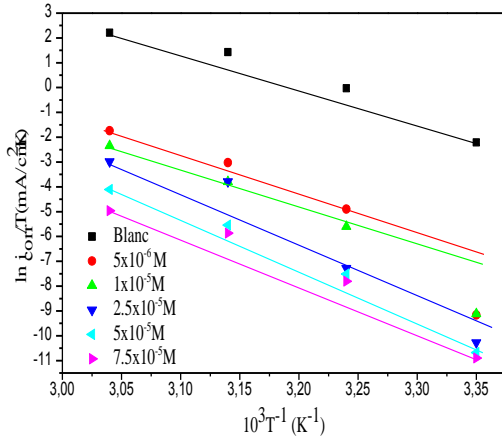


Fig. 4. Alternative Arrhenius plots for mild steel in 1 M HCl in the absence and presence of different concentrations of NO_2AM .

The positive sign of the enthalpy reflects the endothermic nature of the mild steel dissolution process. The negative value of ΔS_a^0 for the inhibitor NO_2AM indicates that the formation of the activated complex in the rate determining step represents an association rather than a dissociation step, meaning that a decrease in disorder takes place during the course of the transition from reactants to the activated complex [6].

D. Adsorption isotherm

Basic information on the interaction between the organic inhibitors and the mild steel surface are obtained from various adsorption isotherms. The most commonly used adsorption isotherms are Langmuir, Temkin and Frumkin isotherms. The experimental data were fitted into various adsorption isotherms but Langmuir isotherm gave the best linear plots. The plots of C_{inh}/θ vs C_{inh} at different temperatures yielded straight lines as shown in Fig. 5.

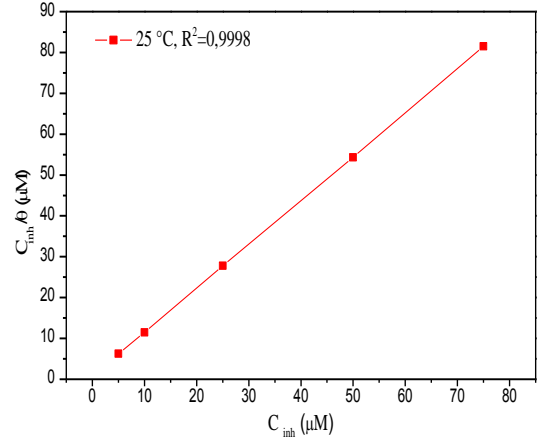


Fig.5. Langmuir adsorption isotherm of NO_2AM on mild steel in 1M HCl at 25°C.

The slope and the correlation coefficient (R^2) values for the Langmuir adsorption plots are listed in Table 4. The correlation coefficient and slope values are near to unity, indicating that the adsorption of this inhibitor on mild steel surface obey Langmuir adsorption isotherm represented by the equation [3]:

$$C_{inh}/\theta = \frac{1}{K_{ads}} + C_{inh} \quad (8)$$

where, C_{inh} is the inhibitor concentration, K_{ads} is the equilibrium constant for adsorption–desorption process. From the intercepts of Fig. 5, the values of K_{ads} were calculated. Large values of K_{ads} obtained for the studied inhibitor imply more efficient adsorption and hence better corrosion inhibition efficiency. Using the values of K_{ads} , the values of ΔG_{ads}^0 were evaluated by using the equation [4]:

$$\Delta G_{ads}^0 = -RT \ln(55.5 K_{ads}) \quad (9)$$

where, R is the universal gas constant, T is the absolute temperature in K, and the numerical value 55.5 represents the molar concentration of water in acid solution. The calculated values of K_{ads} and ΔG_{ads}^0 are given in Table 4. The higher value of K_{ads} associated with strong adsorption of the inhibitor on the surface of mild steel in 1 M HCl. The negative values of ΔG_{ads}^0 indicate that the adsorption of NO_2AM molecule was a spontaneous process and stability of the adsorbed film on the mild steel surface [9]. In the present study the values of ΔG_{ads}^0 varies from -38.98 to -40.77 kJ

mol⁻¹, at different temperatures (303–333 K), signifying that *NO₂AM* adsorb on the mild steel surface in 1 M HCl by physio chemisorption mechanism [13].

TABLE 4 Thermodynamic parameters of adsorption for mild steel in 1 M HCl at different temperatures from Langmuir adsorption isotherm.

Inhibitor	T (°C)	10 ⁵ ×K _{ads} (M ⁻¹)	ΔG_{ads}° (KJ mol ⁻¹)	ΔH_{ads}° (KJ mol ⁻¹)	ΔS_{ads}° (Jmol ⁻¹ K ⁻¹)
<i>NO₂AM</i>	25	0,8092	38,98	22,20	38,82
	35	1,0659	39,60		
	45	1,5786	39,85		
	55	1,8347	40,77		

The standard enthalpy change (ΔH_{ads}°) and standard enthalpy change (ΔS_{ads}°) for the adsorption of inhibitor were determined from the thermodynamic equation:

$$\Delta G_{ads}^{\circ} = \Delta H_{ads}^{\circ} - T\Delta S_{ads}^{\circ} \quad (10)$$

The plot of ΔG_{ads}° versus T was linear (Fig. 6) with the intercept equal to ΔH_{ads}° and slope equal to ΔS_{ads}° as represented in Table 4. It has been reported in literature that an endothermic adsorption process ($\Delta H_{ads}^{\circ} > 0$) is due to chemisorption while an exothermic adsorption process ($\Delta H_{ads}^{\circ} < 0$) may be attributed to physisorption, chemisorption or a mixture of both adsorption processes [12]. There fore, we can conclude that the adsorption of prepared dithiol surfactant on the metal surface is a mixture between physical and chemical process. The ΔS_{ads}° values is positive sign, which mean that, an increase of disorder is due to the adsorption of only one molecule of *NO₂AM* by desorption of more water molecules [6].

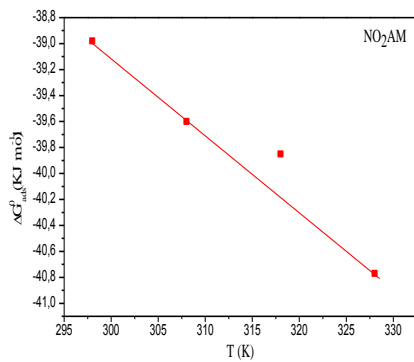


Fig. 6. The relation ship between ΔG_{ads}° and T for *NO₂AM* in 1M HCl medium.

E. Surface analysis by SEM

Scanning electron micrographs (Fig. 7) of the carbon steel surface before and after of the immersion in 1 M HCl with and without addition of *NO₂AM* were taken in order to establish whether inhibition is due to the formation of an organic film on the metal surface. Parallel features on the polished steel surface before exposure to the corrosive solution were observed in Fig. 7A, which are associated with polishing scratches. Figs. 7 B and C show the steel surface after 24 h of immersion in 1 M HCl without and with 7.5×10^{-5} M of *NO₂AM*. The resulting of the high resolution SEM micrograph (Fig. 7B) shows that the steel surface was strongly damaged in the absence of the *NO₂AM* with the increased number and depth of the pits. However, there are less pits and cracks observed in the micrographs in the presence of *NO₂AM* (Fig. 7 C) which suggests a formation of protective film on steel surface which was responsible for the corrosion inhibition. Indeed, *NO₂AM* has a strong tendency to adhere to the steel surface and can be regarded as good inhibitor for steel corrosion in normal hydrochloric medium.

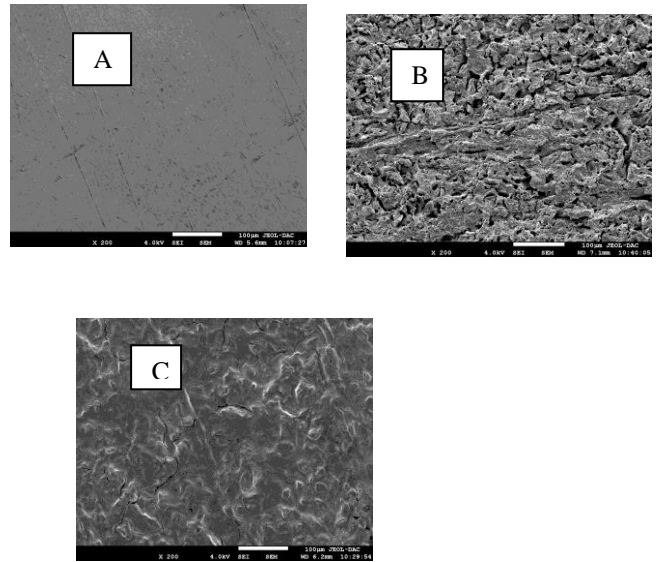


Fig.7. SEM images of mild steel in 1M HCl solution at 25 °C: (A) before immersion (polished), (B) in the absence of *NO₂AM* and (C) in the presence of *NO₂AM* at $7,5 \times 10^{-5}$ M.

III. CONCLUSIONS

- The azomethine *NO₂AM* show good inhibition efficiencies for the corrosion of mild steel in 1 M HCl

solution and the inhibition efficiency increases with increase in concentration of the inhibitor and decreases with the increase in temperature . The maximum inhibition efficiency was observed around 96.06 % at $7.5 \times 10^{-5} \text{M}$ at 25°C .

- Potentiodynamic polarization study revealed that *NO₂AM* behaved as mixed type inhibitor.
- EIS measurements show that charge transfer resistance (R_{ct}) increases and double layer capacitance (C_{dl}) decreases in the presence of inhibitors, which suggest the adsorption of the inhibitor molecules on the surface of mild steel.
- The *NO₂AM* adsorb spontaneously on mild steel surface and their adsorption behavior obey Langmuir adsorption isotherm featuring competitive physisorption and chemisorption mechanisms.
- SEM confirmed the formation of protective film by *NO₂AM* on mild steel surface.

Acknowledgment

This research was financially supported by University of Setif-1-Algeria

References

- [1] S. Issaadi, T. Douadi, S. Chafaa, Adsorption and inhibitive properties of a new heterocyclic furan Schiff base on corrosion of copper in HCl 1 M: Experimental and theoretical investigation Appl. Surf. Sci, Vol. 316, pp. 582-589, 2014.
- [2] S. Issaadi, T. Douadi, A. Zouaoui, S. Chafaa, M.A. Khan, G. Bouet, Novel thiophene symmetrical Schiff base compounds as corrosion inhibitor for mild steel in acidic media, Corros. Sci, vol. 53, pp. 1484–1488, 2011.
- [3] H. Hamani, T. Douadi, D. Daoud, M. Al-Noaimi, S. Chafaa, Corrosion inhibition efficiency and adsorption behavior of azomethine compounds at mild steel/hydrochloric acid interface Measurement, vol. 94, pp. 837–846, 2016.
- [4] H. Hamani, T. Douadi, M. Al-Noaimi, D. Daoud, Electrochemical and quantum chemical studies of some azomethine compounds as corrosion inhibitors for mild steel in 1 M hydrochloric acid, Corros. Sci, vol. 88, pp. 234–245, 2014.
- [5] D. Daoud, T. Douadi, H. Hamani, M. Al-Noaimi, Corrosion inhibition of mild steel by two new S-heterocyclic compounds in 1 M HCl: Experimental and computational study, Corros. Sci, vol. 94, pp. 21-37, 2015.
- [6] D. Daoud, T. Douadi, S. Issaadi, S. Chafaa, Adsorption and corrosion inhibition of new synthesized thiophene Schiff base on mild steel X52 in HCl and H₂SO₄ solutions, Corros. Sci, vol. 79, pp. 50–58, 2014.
- [7] M.Z. Al-Noaimia, H. Saadeh, F. Salim, D. Haddad, I. ElBarghouthi, M. El-khateeb, J. Robert, Syntheses, crystallography and spectroelectrochemical studies of ruthenium azomethine complexes, Polyhedron, vol. 26, pp. 3675–3685, 2007.
- [8] R. Solmaz, Investigation of adsorption and corrosion inhibition of mild steel in hydrochloric acid solution by 5-(4 Dimethylaminobenzylidene) rhodanine, Corros. Sci, vol. 79, pp. 169–176, 2014.
- [9] H. Bentrah, Y. Rahali, A. Chala, Gum arabic as an eco-friendly inhibitor for API 5L X42 pipeline steel in HCl medium, Corros. Sci. vol. 82, pp. 426–431, 2014.
- [10] V. Rajeswari, D. Kesavan, M. Gopiraman, P. Viswanathamurth, Physicochemical studies of glucose, gellan gum, and hydroxypropyl cellulose—Inhibition of cast iron corrosion, Carbohydr Carbohydr, Polym. vol. 95, pp. 288–294, 2013.
- [11] S. Dahiya, S. Lata, R. Kumar, O. Singh, Comparative performance of Uroniums for controlling corrosion of steel with methodical mechanism of inhibition in acidic medium, Part1 Journal of Molecular Liquids, vol. 221, pp. 124–132, 2016.
- [12] N. Kıcır, G. Tansu, M. Erbil, T. Tüken, Investigation of ammonium (2,4-dimethylphenyl)-dithiocarbamate as a new, effective corrosion inhibitor for mild steel, Corros. Sci. vol. 105, pp. 88–99, 2016.
- [13] Z. Tao, S. Zhang, W. Li, B. Hou, Corrosion inhibition of mild steel in acidic solution by some oxo-triazole derivatives, Corros. Sci. vol. 51, pp. 2588–2595, 2009.